

Template Potential Technique in Application to High-Current Beam Simulation

Leonid G. Vorobiev and Richard C. York

National Superconducting Cyclotron Laboratory
Michigan State University
East Lansing, MI 48824-1321, USA

Abstract. Self-potentials and fields of charged particle beams are found by the template potential algorithm. The approach is based on a discrete representation by auxiliary macro-elements or templates of the charge density distribution. Superposition of the potentials and fields including image forces for each template is used to reproduce the total potential and field of the original charge distribution within a conducting boundary. The technique is fast and especially useful for the simulation of charged particle beam dynamics in accelerators, when the Poisson solver is being used repeatedly. Applications to space charge beam simulation are presented.

1 Introduction

To find a numerical solution of the Poisson equation within a region \mathcal{R} ,

$$\Delta u(\mathbf{x}) = -4\pi\rho(\mathbf{x}) \quad \text{for } \mathbf{x} = (x, y, z) \in \mathcal{R}$$

with specified conditions on the boundary $\partial\mathcal{R}$, such grid numerical methods, as Fast Poisson Solvers, are often employed. These algorithms are based on the Fast Fourier Transform (FFT) or cyclic reduction for simple regions and multi-grid algorithms for more complicated boundary shapes. These techniques derive the grid potential $u(\mathbf{x})$ ($\mathbf{x} = (x, y, z)$) and field $E_{x,y,z}$ from a grid density $\rho(\mathbf{x})$ assumed known apriori by solving a set of finite-difference equations. The results usually have an accuracy of $\psi(h) = O(h^2 = h_x^2 + h_y^2 + h_z^2)$ (where $h_{x,y,z}$ are the mesh sizes). These solvers are in common use. See, e.g., [1] and references therein.

During charged particle beam simulation, at each step of the integration of the motion equations, only the coordinates of N_p macro-particles are known. The spatial grid charge density $\rho(\mathbf{x})$ is derived from the position of the beam particles. Since the reproduction of the grid density influences both the speed and the accuracy $\psi_\Sigma = \psi(h, N_p)$ of the calculated potential [2, 3], we present an alternative fast Poisson Solver approach to find self potential and field from macroparticle coordinates.

The new formulation is based on the template potential concept [4, 5] for reconstruction of the total potential of a charged particle beam in the presence of conducting boundaries. This approach allows a significant reduction in the number of macroparticles, N_p , and a sparser spatial grid without concomitant loss of accuracy.

The technique may be used for either envelope or PIC models in either two-dimensional (2D) or three-dimensional (3D) geometries. The template technique has been verified by independent algorithms and shown to be fast and accurate and to be appropriate for many practical space charge related applications.

2 Green's Function, Moment Method and Templates

Analytical and semi-analytical methods. A potential $u(\mathbf{x})$ generated by a charge density distribution $\rho(\mathbf{x})$ inside a volume \mathcal{R} with specified boundary conditions on $\partial\mathcal{R}$ can be represented via the Green's function [6]:

$$u(\mathbf{x}) = \int_{\mathcal{R}} \rho(\mathbf{x}') G(\mathbf{x}, \mathbf{x}') d\mathbf{x}' + \frac{1}{4\pi} \int_{\partial\mathcal{R}} [G(\mathbf{x}) \frac{\partial u(\mathbf{x}, \mathbf{x}')}{\partial n'} - u(\mathbf{x}) \frac{\partial G(\mathbf{x}, \mathbf{x}')}{\partial n'}] ds'$$

For free space, the potential $u(\mathbf{x})$ can be expressed by a simple Green's function of the form $G_{free}(\mathbf{x}, \mathbf{x}') = 1/|\mathbf{x} - \mathbf{x}'|$. Difficulties arise in the presence of a conducting boundary, where it is necessary to fit the solution u to boundary constraints.

For Dirichlet boundary conditions (throughout this paper we will consider this case) the Green's function $G = G_D$ must satisfy $G_D|_{\partial\mathcal{R}} = 0$, and the solution becomes:

$$u(\mathbf{x}) = \int_{\mathcal{R}} \rho(\mathbf{x}') G_D(\mathbf{x}, \mathbf{x}') d\mathbf{x}' - \frac{1}{4\pi} \int_{\partial\mathcal{R}} u(\mathbf{x}) \frac{\partial G_D(\mathbf{x}, \mathbf{x}')}{\partial n'} ds' \quad (1)$$

However, in the absence of simple geometries, the Green's function approach is difficult, limiting its applications. The representation of G_D in cylindrical coordinates to meet boundary conditions, uses the Fourier-Bessel series ([6], p. 116). Therefore, as a practical manner, the Green's function approach is limited to only simple beam distributions and surface $\partial\mathcal{R}$ geometries.

Nevertheless the idea of the Green's function can be employed for numerical Poisson solvers, appropriate for rather general beam distributions and boundary shapes. In the moment method [7], the Green's function formulation is used as a part of computational technique, where the total potential is represented as $u_{total}(\mathbf{x}) = u_{free}(\mathbf{x}) + u_{image}(\mathbf{x})$, $\mathbf{x} \in \mathcal{R}$ satisfying on the boundary $u_{total}|_{\partial\mathcal{R}} = 0$:

$$u_{total}(\mathbf{x}) = \int_{\mathcal{R}} \rho(\mathbf{x}') G_{free}(\mathbf{x}, \mathbf{x}') d\mathbf{x}' + \int_{\partial\mathcal{R}} \sigma_{image}(\mathbf{x}') G_{free}(\mathbf{x}, \mathbf{x}') ds' \quad (2)$$

The potential u_{free} is produced by the charge density ρ in free space with $G_{free}(\mathbf{x}, \mathbf{x}')$. The corresponding image-potential, $u_{image}(\mathbf{x})$, defined by σ_{image} is found from a set of equations $||A|| \sigma_{image} = -u_{free}$ that satisfy the constraint $u_{total}(\mathbf{x})|_{\mathbf{x} \in \partial\mathcal{R}} = 0$ on the conducting surface. Thus, the difficulty in the construction of the proper Green's function G_D for complex geometries is replaced by finding the image density from a set of equations.

Now the moment method with some modifications is known as the charge density method with numerous applications in, e.g., ion optics [8]. Both methods are slower than contemporary grid methods, but can be used in situations in which rapid grid algorithms may be difficult to employ.

Templates. In a previous paper [4], we introduced a numerical method, called the slice algorithm, based on the use of the template potential concept for space charge calculations of a 3D bunched beam. The beam bunch is represented by charged, infinitesimally thin disks, or slices, and the total beam potential is found by the superposition of the potentials from all slices.

The space charge potential of an individual slice of radius R_{slice} within a conducting boundary is found by the moment method (2). Then, the matrix $||A||$ is calculated, σ_{image} is derived from the set of equations, and the total potential u_{total} obtained from:

$$u_{total}^{slice}(\mathbf{x}, S(z)) = u_{free}^{slice}(\mathbf{x}, S(z)) + u_{image}^{slice}(\mathbf{x}, S(z)) \quad (3)$$

where $S(z)$ is a shape function which defines the longitudinal z -profile of the beam for the case of round slices. For elliptical slices, there are two shape functions $S_{x,y}$, which determine the z -profiles. Fig. 1 illustrates the moment method.

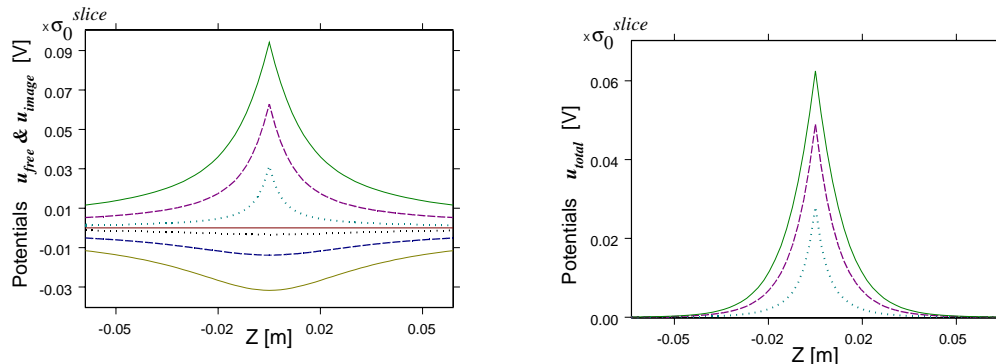


Fig. 1. Template potentials produced by three charged slices of different radii within a conducting beam pipe 4 cm in diameter respectively. Left: $u_{free}(\mathbf{x})$ (positive) and $u_{image}(\mathbf{x})$ (negative) with $\mathbf{x} = (0, 0, z)$, plotted with dotted, dashed and solid lines for slices of 1, 2 and 3 cm in diameter. Right: The corresponding total potentials $u_{total} = u_{free} + u_{image}$ for each slice respectively.

As an illustration, for the case of free space, the potential from a charged disc may be evaluated by the formula:

$$u_{free}(x_0, y_0, z_0) = \int_0^{2\pi} \int_0^{R_{slice}} \frac{\sigma^{slice}(r, \phi) \cdot r dr d\phi}{\sqrt{(r \cos \phi - x_0)^2 + (r \sin \phi - y_0)^2 + z_0^2}}$$

In the case of radial symmetry, a simple analytical representation exists, reducing this formula to: $u_{free}^{slice}(x = 0, y = 0, z) = 2\pi\sigma_0^{slice}(\sqrt{(R_{slice}^2 + z^2)} - |z|)$. All numerically obtained free-space potentials in Fig. 1, coincide with this formula.

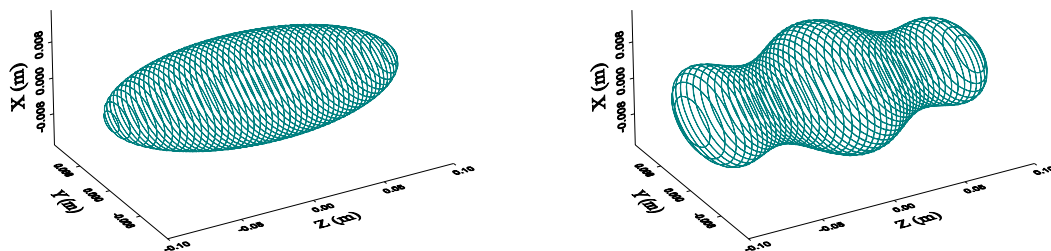


Fig. 2. Two possible 3D beams within a conducting beam pipe 4 cm in diameter represented by $N_s = 50$ slices. Left: Ellipsoid-like beam bunch with semi-axes $R_0 \times R_0 \times z_m = 1 \text{ cm} \times 1 \text{ cm} \times 10 \text{ cm}$ and the shape function $S(z) = R_0 \sqrt{1 - (z/z_m)^2}$. Right: Beam bunch with more general longitudinal variation.

For this specific case all slices were assumed to have constant transverse density $\sigma^{slice}(r) \equiv \sigma_0^{slice}$. The potential for each template satisfies the zero potential boundary conditions and therefore, the superposition of all N_s slices representing the total beam bunch satisfies the Poisson equation. In Fig. 2 are shown two possible bunched beam geometries. In both cases, the beam was assumed to have a total charge of 10^{-11} C and be contained in a conducting chamber 4 cm in diameter. The potentials u_{total}^{bunch} shown in Fig. 3 were obtained by superposition of the potentials of $N_s = 50$ slices, representing the bunch. These N_s slice potentials were found by appropriate scaling and interpolation of the tabulated template potentials.

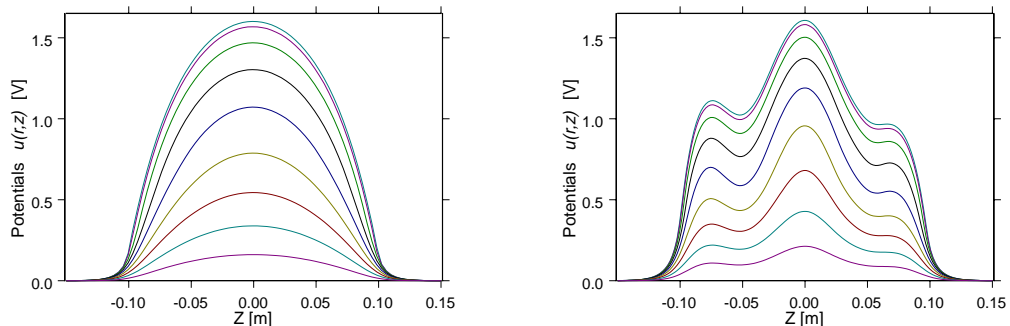


Fig. 3. Potentials $u(x, y, z)$ of bunched beams from Fig. 2 (left and right correspondingly) as a function of longitudinal position, z , for different radii $0 \leq r = \sqrt{x^2 + y^2} \leq R_{cyl}$, with $2R_{cyl} = 4$ cm. (See [9], p. 407 for comparison).

3 Templates for Arbitrary Beams.

The template approach can be used for variable transverse charge distributions and elliptical beam shapes common to quadrupole focusing channels. However, the beam is assumed centered within the conducting chamber.

A general two-dimensional model of the charge density, σ^{slice} , for templates is based on the concept of equivalent beams [9–11]:

$$\sigma^{slice}(x, y, p) = \sigma_m(p) \left\{ 1 - \frac{x^2}{x_m^2(p)} - \frac{y^2}{y_m^2(p)} \right\}^p \quad (4)$$

where $x_m(p)$, $y_m(p)$ are maximal slice coordinates dependent on the parameter p . The rms size may be found from [11]:

$$\langle x^2 \rangle (p) = \frac{\int_{x,y} x^2 \sigma^{slice}(x, y, p) dx dy}{\int_{x,y} \sigma(x, y, p) dx dy}$$

In Fig. 4, rms-matched 2D charge density distributions are plotted. For $p > 0$ the densities are maximum in the center going to zero near the edge. For $p = 0$, the charge density is constant, and for $p < 0$ hollow beams may be represented. For $p \rightarrow \infty$ the charge density is Gaussian [11]. Thus, this approach allows the representation of a broad range of possible charge densities $\sigma^{slice}(x, y, p)$ with rms-matched transverse dimensions.

The rms sizes for beams of elliptical symmetry are given by

$$\langle x^2 \rangle (p) = \frac{\kappa^2 r_m^2 (p)}{2(p+1)} \quad \text{and} \quad \langle y^2 \rangle (p) = \frac{\kappa^{-2} r_m^2 (p)}{2(p+1)} \quad (5)$$

where the semiaxes are $a_x = \kappa r_m (p)$, $a_y = \kappa^{-1} r_m (p)$ with κ being the aspect ratio.

For the case of non-round ($\kappa \neq 1$) beams, it is necessary to calculate the off-axis potentials only for the first quadrant: $\phi \in [0, \pi/2]$. (See Fig. 4.) We found the template potentials

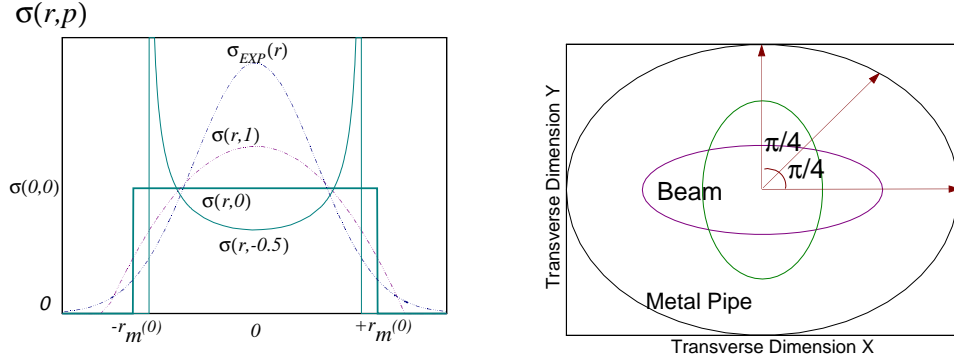


Fig. 4. Left: Rms-matched charge densities $\sigma(r, p)$ as functions of r for different “ p ”. Right: Slice within elliptical conducting boundaries. For elliptical symmetry there will be horizontal and vertical shape functions $S_{x,y}(z)$. See section 4.

along three rays ($\phi = 0, \pi/4, \pi/2$) to be sufficient to interpolate potentials for intermediate ϕ values. Further 10 – 15 different aspect ratios (κ) were found to provide good accuracy for possible transverse beam configurations.

4 Beam Simulation, Using Templates

For the simulation of charged particle beams with significant space charge effects, either rms envelope equations or step-by-step PIC codes may be used. The envelope formalism though computationally fast, is appropriate only for beams with elliptical symmetry propagating through a linear focusing channel in the absence of image forces. The PIC methods are significantly slower, but accommodate arbitrary beam particle distributions, conducting chamber geometries, and focusing structures. The template technique may be applied with different degrees of generality to bridge the gap between rms envelopes and general PIC formulations:

4.1 Extension of 2D and 3D RMS Envelope Equations.

In [11] it was shown how using the template technique the 2D rms envelope formalism [9, 12] can be extended to include the effects of a conducting elliptical chamber. In this context, charged cylinders, instead of disks, are used as templates. The difference between the more complete template approach and that presented by the free space KV formalism is most

pronounced for elliptical boundaries with large aspect ratios. The rms envelope equations for $a_{x,y,z}$, may be also generalized for 3D ellipsoid-like beam bunch:

$$a''_{x,y,z} + K_{x,y,z}a_{x,y,z} - \frac{\varepsilon_{x,y,z}^2}{a_{x,y,z}^3} - F_{x,y,z}^{sc} = 0 \quad (6)$$

where $\varepsilon_{x,y,z}$ are rms emittances, $K_{x,y,z}$ is the linear focusing and $F_{x,y,z}^{sc}$ the space charge force (see [12], p. 278).

However, with the inclusion a conducting boundary, equation (6), assuming linear space charge forces in free space, is not valid. In the presence of conducting walls, the behavior of the space charge forces becomes strongly non-linear even for an ideal ellipsoid [9, 13] or non-ellipsoidal beam, as shown in Fig. 5. However, the template potential method may be

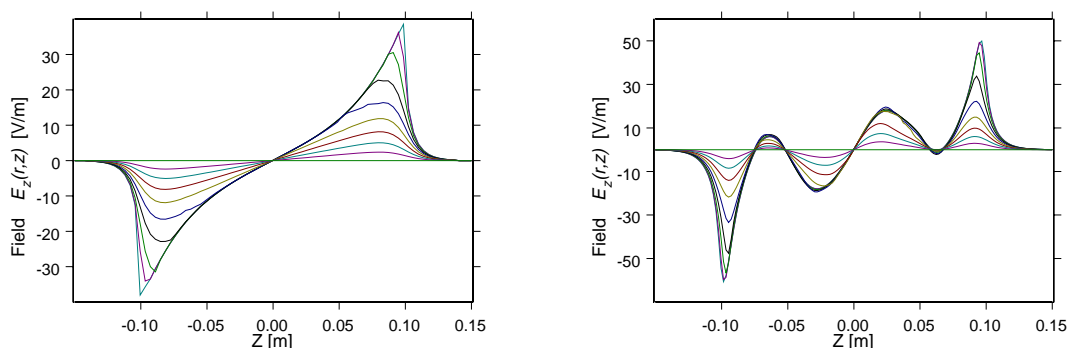


Fig. 5. Longitudinal space charge fields $E_z(x, y, z) = -\partial u / \partial z$ as a function of z , at different radii $0 \leq r = \sqrt{x^2 + y^2} \leq R_{cyl}$. Left: E_z for the ellipsoid-like beam. Right: E_z for the arbitrary beam from Fig. 2.

used to correctly obtain the required fields, even for rather general beam distributions and boundary shapes. Both longitudinal F_z^{total} and transverse fields $F_{x,y}^{total}$ may be obtained from the potentials, by averaging and linearization of $F_{x,y,z}^{total}$. Substitution of this result in lieu of $F_{x,y,z}^{sc}$ in (6), provides a more self-consistent model.

4.2 3D Non-Ellipsoidal Beam.

Arbitrary beams, like that of Fig. 2 (right), may not be appropriately accommodated by an envelope model. We need to include macro-particles $\{\mathbf{x}_i\}$, $i = 1, \dots, N_p$ in the model. In this case, the template approach may again be applied to general beam distributions and conducting boundaries. The transverse rms beam dimensions $\langle x^2 \rangle^{1/2}(z)$ and $\langle y^2 \rangle^{1/2}(z)$, as functions of the longitudinal coordinate, z , are calculated. The shape function $S_{x,y}(z)$ is then found from (5) for a specific p . Previous analysis [11] has shown that for $0 < p < 3$ the result is not sensitive to the precise form of $S_{x,y}$. See Fig. 6. The space charge fields $E_{x,y,z}^{total}$ are derived from $u_{total}(x, y, z)$, $u_{total}(x \pm h_x, y \pm h_y, z \pm h_z)$ and define the space charge forces $\mathbf{F}^{total} = F_{x,y,z}^{total}$ on each particle. The integration of the motion equations:

$$\mathbf{x}_i''(s) + \mathbf{F}^{ext}(\mathbf{x}_i, s) - \mathbf{F}^{total}(\mathbf{x}_i, s) = 0 \quad (7)$$

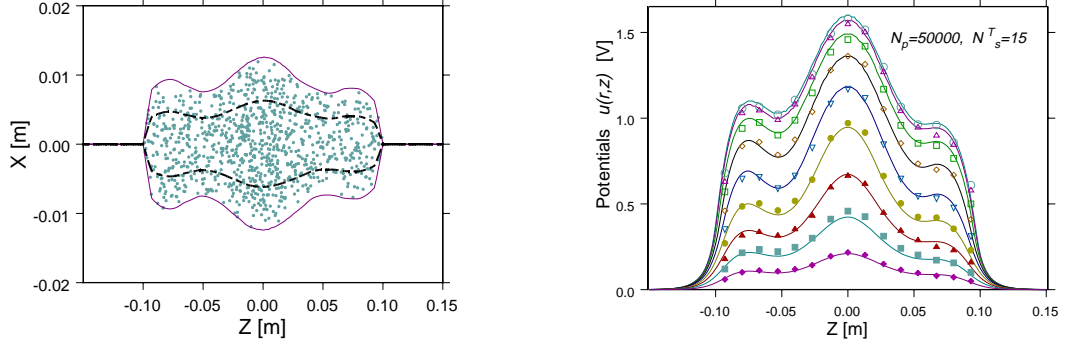


Fig. 6. Left: 3D bunched beam from Fig. 2 (right) within a conducting chamber of radius $R_{cyl} = 2$ cm, showing the macroparticles ensemble in ZX plane. The dashed line shows the rms beam size and the solid line corresponds the actual beam shape $S(z)$. Right: Potentials, found by the sub-3D Poisson Solver as a function of z , at different radii, $0 \leq r = \sqrt{x^2 + y^2} \leq R_{cyl}$. The solid lines are the solutions of the template technique and symbols are from the sub-3D Poisson Solver for $N_z^T = 15$ “thick” slices.

can be implemented in a self-consistent manner even with arbitrary non-linear external forces \mathbf{F}^{ext} . After that, new coordinates $\{\mathbf{x}_i\}$ are found and new rms-profiles, shape functions, and total potentials obtained [14]. Note, that with this approach explicit calculation of charge density is not required. See Fig. 7.

The number of macroparticles required is relatively small, e.g., $N_p \propto 10^4$, since the macroparticles are used only to generate the shape function, $S_{x,y}(z)$, rather than the spatial density $\rho(\mathbf{x})$. In contrast, other PIC approaches such as those using cloud-in-cell (CIC) density algorithms, require $10^6 - 10^7$ macroparticles. As a result, the integration of equations (7) is very fast.

4.3 Sub-3D Poisson Solver for General Beam Simulation.

The space charge potential in the region \mathcal{R} , satisfying zero boundary conditions at $\partial\mathcal{R}$ may be found from the 3D Poisson equation, which can be re-written as:

$$\frac{\partial^2 u}{\partial x^2} + \frac{\partial^2 u}{\partial y^2} = -4\pi\rho(x, y) - \frac{\partial^2 u}{\partial z^2}$$

Introducing the corrected charge density [5], we obtain:

$$\rho_{corr}(x, y, z) = \rho(x, y, z) + \frac{1}{4\pi} \frac{\partial^2 u}{\partial z^2} \quad (8)$$

Then the standard Poisson equation may be re-written as:

$$\frac{\partial^2 u}{\partial x^2} + \frac{\partial^2 u}{\partial y^2} = -4\pi\rho_{corr}(x, y) \quad (9)$$

Note, that the series of 2D solutions of (9) could be used to obtain the solution of the original Poisson equation if the term $\partial^2 u / \partial z^2$ would be known. Dividing the beam along

the longitudinal, z , axis by N_z^T “thick” slices, we can rewrite the Poisson equation (9) and for each “thick” slice $z^T \in [z - H_z^T, z + H_z^T]$ a 2D Poisson equation is solved with the new density ρ_{corr} :

$$\rho_{corr} = \frac{\rho_{2D}(x, y, z^T)}{H_z^T} - \frac{1}{4\pi} \frac{\partial E_z}{\partial z} \quad (10)$$

Instead of $\partial^2 u / \partial z^2$ in (8) we substitute in (10) the driving term $-\partial E_z / \partial z$, obtained from the template technique solution for the same boundary constraints. Thus, the 2D Poisson solver for (9)-(10) for each “thick” slice finds the transverse self-potentials and electric fields $E_{x,y}$ with all possible generality, whereas the longitudinal fields E_z are supplied by the template technique. See Fig. 6. The corresponding space charge forces $F_{x,y,z}^{total}$ are substituted into the equation (7) for trajectories integration.

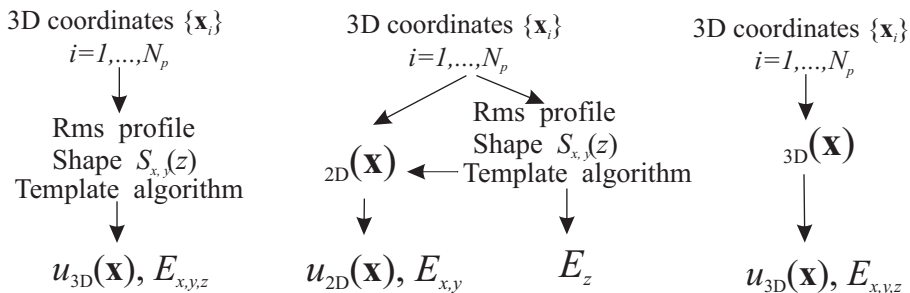


Fig. 7. Space charge calculations by different methods for one step of integration of the 3D beam motion equations. Left: Method from section 4.2. Middle: Sub-3D Poisson Solver from section 4.3. Right: Regular 3D Solver.

Note, that the generation of the transverse forces is separated from the longitudinal forces. The derivative $\partial E_z / \partial z$ participates in each of the 2D Solvers by correcting the 2D charge density. Without inclusion of the driving term $\partial^2 u / \partial z^2$ the calculation of $E_{x,y}$ would be in error [5]. Fig. 7 illustrates a step of integration using the sub-3D and a general 3D Poisson Solvers.

5 Templates as Special Functions

Tabulation, parameterization, interpolation. The tabulation of the template potentials prior to beam simulation follows the principle used for other special functions that do not have a simple analytical representation. During the actual space charge simulations, the template data is extracted from the table with appropriate scaling and interpolation. The storage requirements for the template table can be minimized. Since each template potential represents an even function, it is necessary to store only half of them, say $u(x, y, z)$ for $z > 0$. See Fig. 1. In addition, the template data could be parametrized and only the resulting coefficients stored.

The number of templates required depends on the geometry of the problem. For the axially symmetric beam of Fig. 2, only 10 different radii were required. For each such template, 10 off-axis potentials should be calculated, resulting in a total of 100 templates. For cases with less symmetry, e.g., for beam and boundary with elliptical symmetry of Fig. 4 about of

3000 templates are required with the increase from necessary different azimuthal positions ($3\times$) and aspect ratios ($10\times$). Thus, the table of templates is of a moderate size. All intermediate quantities are obtained by interpolation and scaling of the tabulated data. For 2D cases, when there is no dependence on z , the memory demands are an order of magnitude less.

Limitations of the template formalism. The accuracy of the sub-3D Poisson solver approaches is that of the general 3D PIC models. Nevertheless, the template formalism is not completely self-consistent because the pre-calculated data may not adequately reflect all possible evolutions of the particle distribution. Since the transverse 2D analysis can be used for arbitrary densities $\rho_{2D}(x, y,)$, the 2D problems are solved with all possible generality. The lack of self-consistency is in the replacement of $\partial^2 u/\partial z^2$ by $\partial E_z/\partial z$ in (10).

Nonetheless, the quantitative analysis in [10, 11] showed that for a large class of density distributions $\sigma(x, y, p)$ there is a relatively weak sensitivity of the longitudinal E_z fields to the details of transverse charge densities. As the result, the space charge fields: $E_{x,y}$ found from a series of 2D problems (9) and E_z , supplied by the slice algorithm, provide an accurate representation of space charge forces.

For beams, whose transverse densities may be described analytically (4), the template formalism is appropriate. However, for cases where the beam bunch has, e.g., isolated off-axis clusters, the template formalism is not appropriate and a general 3D PIC method should be employed.

6 Discussion and Conclusions

The template technique is oriented toward repeated calculations, e.g., for charged particle beam dynamics simulation. For those situations, where the beam pipe sizes are fixed or only slightly varying and the beam is “well-behaved” in the sense discussed above, the templates procedure significantly reduces simulation computational time. The verification of the method has shown a good agreement with general 3D grid solvers for a large class of charge density distributions. The proper inclusion of changing boundaries would require additional pre-calculated template data. This might be justified if only a few possible geometries are required. However, when the boundaries are complicated and/or changing significantly, and if the beam distribution is arbitrary (i.e. off-set from the axis, disintegrated into clusters, etc.) the template technique is likely inappropriate and conventional grid methods are recommended.

Preliminary numerical studies provide confidence that the template formalism is an efficient method for fast space charge calculations in the presence of conducting boundaries. It allows the extension of 2D and 3D beam rms-envelope equations including conducting boundaries. It provides a transition to self-consistent rather general sub-3D PIC, that is significantly faster than conventional 3D PIC formulations.

Acknowledgment

This work was supported by the U.S. Department of Energy under Contract No. DE-FG02-99ER41118.

References

1. Press, W.H., Teukolsky, S.A., Vetterling, W.,T., Flannery B.P.: Numerical Recipes. Second Edition. Cambridge (1992).
2. Hockney, R.W., Eastwood, J.W.: Computer Simulation Using Particles. McGraw-Hill, (1981).
3. Birdsall, C.K., Langdon, A.B.: Plasma Physics via Computer Simulation. McGraw-Hill (1985).
4. Vorobiev, L.G., York, R.C.: Calculations of Longitudinal Fields of High-Current Beams within Conducting Chambers. In: Luccio, A., MacKay, W. (eds.): Proc. 1999 Particle Accelerator Conf., New York, IEEE, Piscataway, NJ (1999) 2781-2783.
5. Vorobiev, L.G., York, R.C.: Space Charge Calculations for Sub-Three-Dimensional Particle-In-Cell Code. Phys. Rev. ST Accel. Beams **3**, 114201 (2000).
6. Jackson, J.D.: Classical Electrodynamics. Wiley, New York (1975).
7. Harrington, R.F.: Field Computation by Moment Methods. Macmillan Company, New York (1968).
8. Szilagy, M.: Electron and Ion Optics. Plenum Press, New York (1988).
9. Reiser, M.: Theory and Design of Charged Particle Beams. Wiley, New York (1994).
10. Vorobiev, L.G., York, R.C.: Slice Algorithm – Advanced Version. Michigan State University Report MSUCL-1191, East Lansing (2001).
11. Vorobiev, L.G., York, R.C.: Method of Template Potentials to Find Space Charge Forces for High-Current Beam Dynamics Simulation. In: Lukas, P., Webber, S. (eds.): Proc. 2001 Particle Accelerators Conf., Chicago, IEEE, Piscataway, NJ (2001) 3075-3077.
12. Wangler, T.P.: Principles of RF Accelerators. Wiley, New York (1998).
13. Vorobiev, L.G., York, R.C.: Numerical Technique to Determine Longitudinal Fields of Bunched Beams within Conducting Boundaries. Michigan State University Report MSUCL-1117, East Lansing (1998).
14. Vorobiev, L.G., York, R.C.: to be published.